

# The Response of Northern Hemisphere Atmospheric Circulation to the Northward Migration of Tropical Forcing

JaYeon Moon<sup>1</sup>, Bin Wang<sup>2</sup> and Won-Tae Kwon<sup>1</sup>

<sup>1</sup>*Climate Research Team, National Institute of Meteorological Research,  
Korea Meteorological Administration, Seoul, Korea*

<sup>2</sup>*Department of Meteorology, University of Hawaii, Honolulu, USA*

(Manuscript received 18 June 2007; in final form 13 August 2007)

## Abstract

The interannual variability of sea surface temperature (SST) in the tropics induces changes in global-scale atmospheric circulation not only in seasonal-to-interannual time scale but also in sub-seasonal time scale such as Madden-Julian Oscillation (MJO). The present study investigates the response of Northern Hemisphere (NH) atmospheric circulation to the tropical forcing in order to explain the mechanism of the features found from the interannual variability of tropical convection and extratropical circulation in intraseasonal time scale which showed distinctive differences between warm and cold episodes of El Niño and Southern Oscillation (ENSO). The tropical convection associated with MJO are found to have latitudinal and longitudinal movement as the western Pacific warm pool evolves by the interannual variability of SST. As a mid-latitude response, the extratropical circulation experiences large contrast in the magnitude of variability between the cold and warm episodes of ENSO. To explain the cause of the magnitude difference in the NH atmospheric circulation between opposite phases of ENSO, several tropical SST forcing experiments are performed. The sensitivity experiments forced by dipole SST anomalies with maximum centered at the equator and 10 degree north with the longitudinal locations varying from the Indian Ocean to the central and eastern Pacific are integrated with 8 ensemble members. The simulated mid- to high-latitude geopotential height is shown to be in good accordance with the observation especially over the Asia-Pacific-North America sector and the magnitude of the extratropical variability is enhanced when the tropical forcing was located to the north. From the experiments, it is confirmed that the atmospheric variability in the extratropics is largely contributed by the latitudinal migration of the tropical forcing as well as the changes in longitudinal location.

**Key words:** MJO, ENSO, Tropical forcing, Experiment, Northward Migration, Extratropical response

## 1. Introduction

Sea surface temperature (SST) fields are reflection of the thermal condition of the upper layer in the ocean and their anomalies are formed and maintained by quite complicated thermal and physical processes (Frankignoul, 1985). It is suggested that the influence of SST on atmosphere can be divided by three mechanisms: (1) formation of thermal pattern through the change of latent and sensible heat fluxes,

(2) formation of Rossby wave through the change of vorticity, and (3) generation of thermal anomaly through the stretching of vorticity and meridional movement (Shukla, 1981). Among the three mechanisms, many studies (Opsteegh and Van den Dool, 1980; Hoskins and Karoly, 1981; Wallace and Gutzler, 1981; Simmons, 1982; Shukla and Wallace, 1983; Branstator, 1983) have used the quasi-stationary Rossby wave dispersion theory to show that the tropical SST anomalies have a significant influence on mid-latitude circulation through the teleconnection pattern called Pacific/North American (PNA) (Wallace and Gutzler, 1981). Since the heating anomalies in the tropics are not uniform in space, the temporal and spatial variations of heat sources in the tropical region might have a significant impact on global climate systems not only in low latitudes

---

Corresponding Author: JaYeon Moon, Climate Research Team, National Institute of Meteorological Research, Korea Meteorological Administration, Shindaeabang-2dong, Dongjak-gu, Seoul, Korea.  
Phone : +82-2-846-2852, Fax : +82-2-846-2853  
E-mail: mjy@kma.go.kr

but also in high latitudes (Nitta, 1987). Over the past three decades it has become increasingly clear that a portion of the atmospheric circulation variability in both the tropics and extratropics is coupled to large-scale changes in tropical heating over a broad frequency range (Kiladis and Weickmann, 1992). Madden and Julian (1972) found out that there are strong intraseasonal fluctuations in tropical convection and circulation associated with an eastward-propagating wave in the vicinity of the equator with an irregular period in the range of 30–60 days. This is well known as the Madden-Julian Oscillation (MJO). Weickmann (1983) and Lau and Phillips (1986) have also noted an apparent relationship between large-scale eastward-propagating tropical OLR anomalies and extratropical circulation modes in intraseasonal time scale. In their study, space-time evolution of extratropical wavetrain is found to be coherent with the tropical dipolar convection. The strongest convection over Indonesia/central Pacific is found to be in approximate quadrature with the peak phase of the Eurasia and Pacific-North America wavetrains. More recent studies have revealed that the life cycle of this wave is tied to global scale anomalies in circulation (Knutson and Weickmann, 1987; Rui and Wang, 1989; Ferranti *et al.*, 1990; Moon and Ha, 2002; Moon *et al.*, 2005).

To explain the mechanism for this close connection, several categories of models have been used ranging from high-resolution atmospheric general circulation models (AGCM) to simple one equation models. For example, the simulation of barotropic models suggests that the extratropical response results from Rossby wave dispersion on the sphere, with the wave source related to the divergent flow in the tropical upper troposphere. It also shows an equivalent barotropic vertical structure in the mid-latitudes. This is consistent with the fact that tropical diabatic heating is primarily balanced by adiabatic cooling due to the upward motion by the upper-level divergence. Among the GCM experiments, Ting and Sardeshmukh (1993) found that the extratropical response to tropical forcing was very sensitive to the basic surrounding state and to the longitudinal position of the tropical forcing with respect

to the climatological waves. Sardeshmukh and Hoskins (1988) have suggested the importance of simulating the upper-level patterns of divergence and convergence accurately by representing a sophisticated thermal and orography forcing and considering the zonal variations of the basic state with the full complexity of a GCM. However, the modeling studies focusing on the response to the tropical heating anomalies associated with MJO are rather few. Ferranti *et al.* (1990) examined the response to the MJO in a simple barotropic model, and found the modeled response in the northern hemisphere resembled some aspects of observed extratropical variations correlated with the OLR fluctuations. Park *et al.* (1995) have examined the impact of MJO-like tropical heating anomalies on the extratropical circulation using a GCM. Using a stationary and propagating forcing in the model, they have obtained that the response to the propagating forcing was weaker and of different phase, indicating that the 40-day period of forced propagation was too short to allow the development of the steady-state response in the extratropics.

In the study of Moon and Ha (2002), life cycles of intraseasonal tropical convection and associated extratropical circulation are compared between warm and cold years of ENSO (El Niño and Southern Oscillation). They found that the interannual variability of the MJO activities over the tropics appear as the movement of the maximum variance centers in meridional direction, while that over the extratropics show as the magnitude difference especially over the Asia-North Pacific-America sectors. That is, the variability of MJO intensifies more to the north (south) during La Niña (El Niño) over the western Pacific which is related with the large (weak) magnitude of variability over the extratropical atmosphere. Moon *et al.* (2005) have verified these observational results by using a coupled GCM (CGCM) dataset. They summarized that even though the coupled GCM simulates the MJO and its connection with the extratropical circulation anomalies quite successfully, simulation of the interannual variability of the MJO and associated extratropical intraseasonal variability was still difficult to achieve.

In the present study, we extend the previous two studies by investigating the cause of the interannual characteristics associated with MJO in the extratropics which were pointed out by the previous two studies (Moon and Ha, 2002; Moon *et al.* 2005). To obtain the extratropical response to the tropical forcing and to simulate MJO-like mode in the tropics, we employ stationary forcing instead of propagating forcing. Since the AGCM still has difficulty in simulating the realistic MJO, we will assume the MJO-like forcing in the tropics, that is, the extratropical response is obtained only by shifting the tropical dipole structure in longitudinal direction without considering the evolution of the convective activity with time. This study will focus on finding the effect of northward migration of the MJO-like forcing anomalies in the tropical region to the circulation anomalies over the Northern Hemisphere (NH) extratropics.

Section 2 briefly explains model and the experiment design used in this study and section 3 shows the observed features of interannual variability of MJO and MJO-associated extratropical variability. Section 4 shows ensemble mean response of the atmosphere to the longitudinally moving MJO-like forcing anomalies. In section 5, the contrasts of mid-latitude atmospheric variability to the meridional displacement of the tropical forcing are explained and section 6 summarizes and discusses the results. In this study, it will be shown that the northward shift of the MJO-like convective activities over the tropical Pacific can give rise to the difference in the magnitude of the variabilities in the NH circulation.

## 2. The Model and Experiments

### a. Model Description

The model used in this study is the version 3 of Community Atmosphere Model (CAM), which is an atmospheric general circulation model that includes the Community Land Model (CLM3), an optional slab ocean model, and a thermodynamic sea ice model, developed by the climate community in collaboration with the National Center for Atmospheric

Research (NCAR). The dynamics and physics in CAM3 have been changed substantially compared to implementations in previous versions. The new atmospheric model includes significant changes to cloud and precipitation processes, radiation processes, and treatments of aerosols. The physics of cloud and precipitation processes have been modified extensively. The modifications include separate treatments of liquid and ice condensate; advection, detrainment, and sedimentation of cloud condensate; and separate treatments of frozen and liquid precipitation. The radiation has been updated with a generalized treatment of cloud geometrical overlap and new treatment of longwave and shortwave interactions with water vapor. More details are explained in Collins *et al.* (2006). The present study uses CAM3 at T42 horizontal resolution, which approximately corresponds to a grid resolution of 2.8° latitude by 2.8° longitude. Twenty-six levels in the vertical are resolved, and the model time step is 20 minutes.

### b. Experiment Design

The atmospheric sensitivity to equatorial SST forcing is examined by prescribing idealized SST anomalies. The GCM experiment is designed with a control of zonally symmetric climate and perturbation by idealized tropical SST anomaly that mimic eastward propagating MJO dipole mode. Given the apparent complexity of a GCM, it should be easier to diagnose the response with a model linearized about a zonally symmetric flow. The horizontal distribution of the heating anomaly used in this study is given by (Ting and Held, 1990),

$$T_A(\lambda, \theta) = A e^{-(\theta/L_y)^2} [e^{-[(\lambda-\lambda_1)/L_x]^2} - e^{-[(\lambda-\lambda_2)/L_x]^2}] \quad (1)$$

The longitudinal and latitudinal scales,  $L_x$  and  $L_y$ , are respectively 30° and 10°, and the amplitude  $A$  is 2.5°C. Series of experiments are designed to establish the sensitivity of the mid-latitude anomaly response to the position of the SST anomaly. The regions of the tropical forcing are described in Table 1 and presented in Figure 1. It was positioned at four

**Table 1.** Experiment Design.

Tropical Forcing (Latitude)		Tropical Forcing (Longitude) (Dipole anomalies: + Shading, - Blank)			
		EXP1	EXP2	EXP3	EXP4
10°S-10°N (_S)	0°-20°N (_N)	20°-80°E	60°-120°E	120°E-180°	180°-120°W
		100°-160°E	140°-200°E	40°-100°E	100°-160°E
Control		Zonally symmetric SST (January Climatology)			

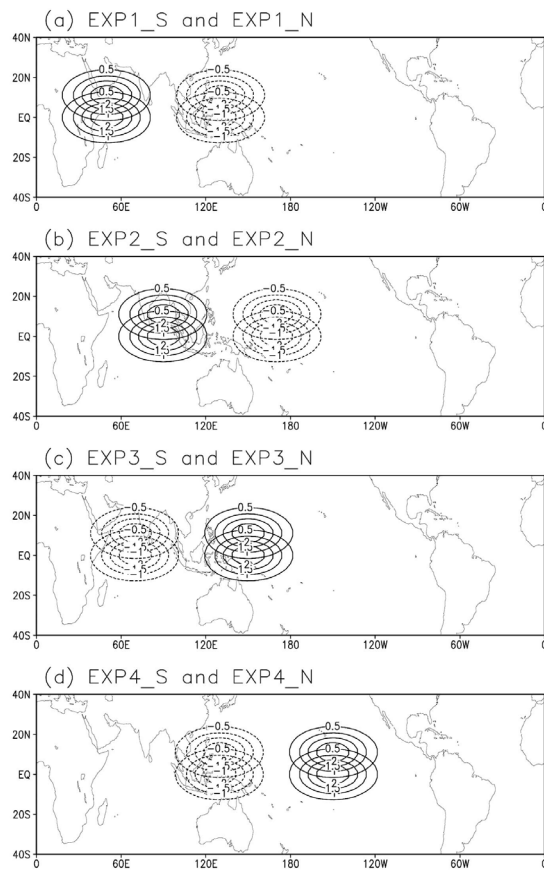


**Fig. 1.** Distributions of sea surface temperature (SST) anomalies used in the MJO-like forcing experiments. Dipole indicates idealized SST anomalies centered at the equator (\_S) and 10 degree north (\_N). Contour intervals are 0.5 °C (Dot: below -0.5 °C, Solid: above 0.5 °C).

different locations spanning the tropical band from the Indian Ocean to the central Pacific with the centers at the equator (\_S) and 10 degree north (\_N), respectively. Ensembles of 8 member AGCM runs forced with the zonally symmetric January SST cli-

matology plus idealized SST anomalies using time-lagging (one day) method are performed. For AGCM experiments, the model response is determined by the 8-member ensemble mean difference between the forced and the control runs. Control run is forced with zonally symmetric SST and every experiments are run in the perpetual mode fixed on the 15th of January with 120-day duration (last 90 days are used). A student's t-test is used to determine the statistical significance of the response.

### c. Data

The observation data are daily mean zonal wind, and geopotential height at the 200 hPa level from NCEP/NCAR (National Centers for Environmental Prediction/National Center for Atmospheric Research) Reanalysis, daily mean OLR (Outgoing Longwave Radiation) from NOAA (National Oceanographic and Atmospheric Administration). The horizontal resolution is 2.5°/2.5° in longitude/latitude and the period is from 1979 to 2000. For the analysis, 21 boreal winters from December to February are taken and the variables are band-pass filtered in 30~60 day time scale using Lanczos filter (Duchon, 1979).

## 3. Interannual variability of MJO and MJO-associated extratropical variability

To describe the contrasting variability of MJO and MJO-associated extratropical circulation during warm and cold phases of El Niño and Southern Oscillation (ENSO) in detail, we have modified Fig. 1 in Moon and Ha (2002)'s study. Fig. 2 shows intra-seasonal variance (ISV) maps of OLR and geopotential height at 200 hPa level (H200). During bor-

real winter, the maximum ISV of OLR (upper left panel) occurs as a longitudinally elongated band from the tropical Indian Ocean to SPCZ (South Pacific Convergence Zone) near 120°W. In the mid- to high latitudes, the maximum variance of H200 (upper right panel) locates over the North Pacific, northeastern America, North Atlantic, and northwestern Europe where the predominant atmospheric low-frequency teleconnection occurs as mentioned in the study of Wallace and Gutzler (1981). The global patterns of OLR ISV anomaly during El Niño are almost the same as La Niña but with opposite polarities. The most distinguishable feature between the El Niño and La Niña is the latitudinal and longitudinal movements of the enhanced intraseasonal convection centers. During El Niño, the ISV is enhanced over the central tropical Pacific and central-eastern Pacific of Southern Hemisphere (SH); while in La Niña, it occurs over Arabian Sea-Bay of Bengal, and Philippine

Sea, which are close to the subtropics. It is noteworthy that ISV of OLR enhances over the tropics, close to the equator during El Niño, while it intensifies close to the subtropics, which locates at the northern side of the climatological mean during La Niña.

Over the mid- to high-latitude, ISV anomalies of H200 have global patterns with reversed polarities between El Niño and La Niña. However, over the Atlantic sector, the decrease of the ISV appears the same in both El Niño and La Niña years. During El Niño, weaker ISV is seen in the mid- and high-latitudes, while in La Niña, the ISV is intensified except in the North Atlantic Ocean.

From the analysis of Fig. 2, we can get a clue that the northward migration of the MJO convective maximum during La Niña events may have resulted in enhancing the wave activity over the mid- to high-latitudes. On the other hand, the weak variance over

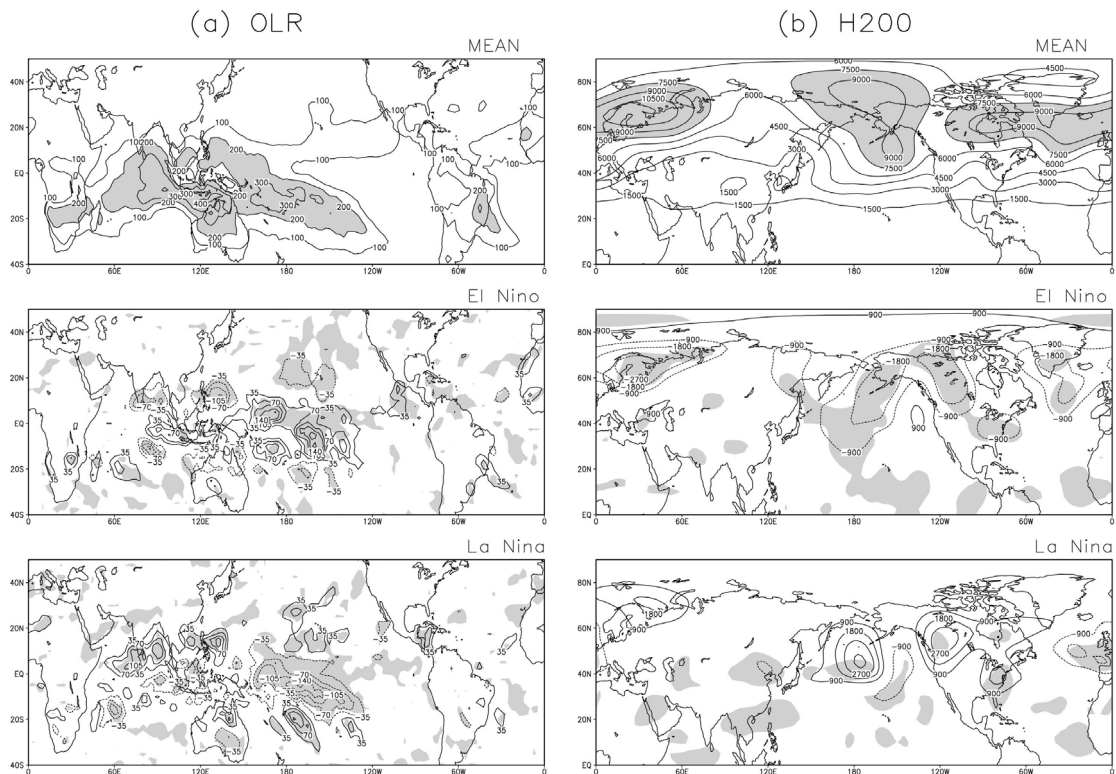


**Fig. 2.** The intraseasonal variance of climatological mean (upper), anomalies from the mean during El Niño years (middle) and La Niña years (bottom) of (a) OLR and (b) 200 hPa geopotential height (H200). Shaded regions in the anomaly map indicate statistically significant regions of 95 % significance level. Units are  $(W/m^2)^2$  for OLR and  $(gpm)^2$  for H200.

the mid- to high-latitude during El Niño may be caused by the active tropical convection which are only trapped at the equator and SH.

#### 4. Response of mid-latitude atmospheric circulation to the eastward evolution of tropical dipole heating

Attempts to verify the role of the longitudinally varying tropical heating on extratropical circulation are conducted with prescribed location-varying SST anomaly along the equator. Our principal purpose is to diagnose the response of the extratropical cir-

lation to the tropical forcing which propagate in phase with each other. Fig. 3 shows the model simulated OLR to the MJO-like forcing centered at the equator along the tropical Pacific together with the observed MJO life cycle map of Fig. 5 in Moon and Ha (2002). As the tropical dipole modes propagate eastward from the Indian Ocean to the central Pacific in MJO time scale, the simulated OLR anomalies induced by SST anomalies form as a north-south and east-west dipole straddling the northern margin of the forcing anomalies in the equatorial Pacific. The OLR anomalies represent quite realistic MJO-like convection and resemble the observed ones as the max-

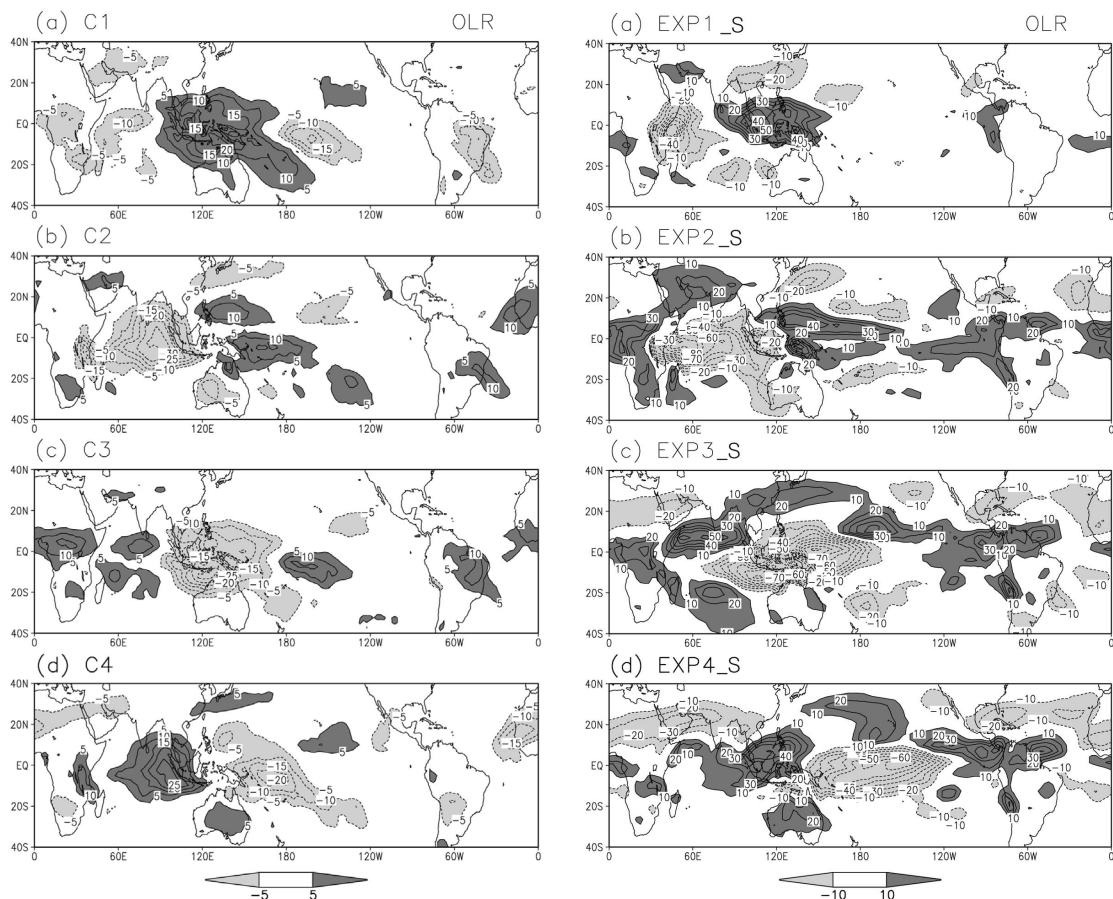


**Fig. 3.** (Left) Composites of outgoing longwave radiation (OLR) formed by EOF1 and EOF2, selecting the days when (a) C1 ( $E2 > S2$ ), (b) C2 ( $E1 > S1$ ), (c) C3 ( $E2 < -S2$ ), (d) C4 ( $E1 < -S1$ ). Contour interval is  $5 \text{ W/m}^2$  and the values greater (less) than  $5$  ( $-5$ )  $\text{W/m}^2$  is shaded. E1, E2: first and second principal component. S1, S2: standard deviation from E1, E2. "-" means opposite sign. (Right) Composites of outgoing longwave radiation (OLR) formed by simulation results of experiment (EXP) 1 to 4. Each figure shows the 8-member ensemble mean difference between the forced and the control runs. Contour interval is  $10 \text{ W/m}^2$  and values greater (less) than  $10$  ( $-10$ )  $\text{W/m}^2$  are shaded.

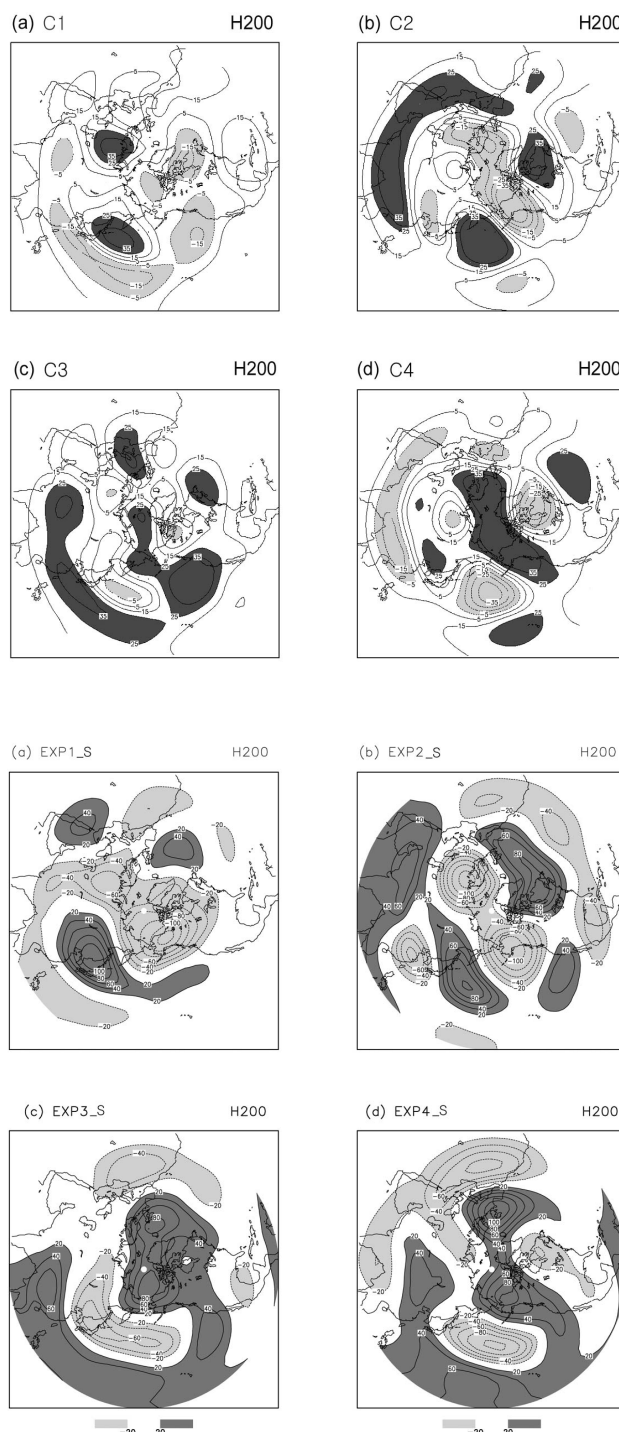


**Fig. 4.** (Upper Panel) Same as Fig. 3, but for the composites of geopotential height at 200 hPa. Contour interval is 10 gpm and the values greater than 25 gpm and lower than -5 gpm are shaded. (Bottom Panel) Same as Fig. 3, but for the composites of geopotential height at 200 hPa from EXP1\_S to EXP4\_S. Contour interval is 20 gpm and the values greater (less) than 20 (-20) gpm are shaded.

imum convection moves from the Indian Ocean (EXP1) to the central Pacific (EXP4).

As to this idealized MJO-like tropical forcing at the equator, Fig. 4 displays the simulated responses of 200-hPa geopotential heights with the observation result of Fig. 6 in Moon and Ha (2002). In EXP1, East Asia is located at the center of anticyclone with the cyclones located to its northeast and southwest directions, which are successfully captured, comparing with the observation. In EXP2, a wave train developed from the Indian Ocean, propagating whole longitude reaching to north Atlantic is found. The locations of cyclonic/anticyclonic anomalies over the NH are in correspondence with the observation. Similar feature from EXP1 and EXP2, but with opposite sign can be detected in EXP3 and EXP4, respectively, indicating the close relationship between the tropics and the extratropics. The wave propagation that elongates from the south of East Asia to the United States are found in EXP3. The tropical forcing at the central Pacific (EXP4) has produced the wave pattern that looks like PNA (Pacific/North America).

From the result of Fig. 4, the upper-level wave patterns of simulation are found to be in good accordance with the observation especially over the Asia-Pacific-North America-Atlantic sector, proving that there exists close relationship between the tropical heating and the extratropical circulation. In Moon and Ha (2002)'s study, we have noted the mirror-image response of the extratropical atmosphere by the opposite phases of tropical convection. The simulated extratropical response from Fig. 4 indicates that a wave-like feature formulated in the NH atmosphere is largely due to the idealized tropical dipole heating anomalies. This result also suggests that the model used in this study is largely reproduces the tropical-extratropical interaction process. Several studies (Geisler *et al.*, 1985; Held and Kang, 1987) have reported an insensitivity of the mid-latitude circulation to the longitudinal displacement of heating anomaly in the equatorial region of the Pacific Ocean. However, the results in our study show the sensitivity in mid-latitude response to the movement of longitudinal tropical forcing.

## 5. Contrasts in the mid-latitude atmospheric variability to the northward migration of MJO-like forcing

As noted by Branstator (2003), the change of position in the anomalous tropical convection may induce a large difference over the extratropical flow. In the present study, we focus on the response of the extratropical atmosphere to the northward migration of the tropical forcing. In the previous chapters, we suggested that the strong (weak) extratropical variability during La Niña (El Niño) may have close connection with the northward (southward) enhancement of MJO variability over the tropical Pacific region. To identify this idea, we have performed sensitivity experiments in which the tropical peak forcing is centered at the equator ( $_{\text{S}}$ ) and 10 degree north ( $_{\text{N}}$ ) with 20 degree latitudinal width. Fig. 5 shows the difference of the extratropical variability forced by the northward migration of tropical heating anomalies. In EXP1, in which the tropical forcing locates over the western part of Indian Ocean shows little enhancement of tropical convective activity by the northward migration of heating anomalies. At the same time, the extratropical variability has no significant change. When the convection is located at the center of the Indian Ocean (EXP2), the model simulates increased tropical variability over the north of the Indian Ocean to the East Asia. However, the decreased variance over the mid- to high-latitude is detected. In EXP3, the increased variance both over the tropics and the extratropics highly resembling the observed features in Fig. 2 during La Niña years. The convective activity is more active through the northern part of the tropical Pacific and the response of the extratropical atmosphere occurs mainly over the north Pacific-north America sectors. In EXP4, the convection is more enhanced over the eastern Pacific with the extension of the regions of enhanced variability in the extratropical height.

Fig. 6 displays the difference of the variability in the upper-level wind. The strong variance is developed at the northern periphery of the enhanced convection and at the south of the intensified extratropical height variability in all four experiments.

These features can be explained by the relationship between the tropics and the extratropics through local Hadley circulation in which the upper-level divergent flow will enhance the westerly flow by coriolis force. The enhanced variability of zonal wind in the mid-latitude is more obvious in EXP3 and EXP4 since the tropical forcing is also more strengthened.

From the result in Fig. 5 and 6, it is obvious when the convection is strengthened more to the north over the tropical Pacific, the strong zonal wind and the vorticity anomalies response and are enhanced over the north Pacific-North America sectors. Hoerling and Ting (1994) also suggested that the extratropical vorticity transients, which are influenced by tropical forcing, are the primary mechanisms in maintaining stationary wave anomalies over the Pacific/North America (PNA) region during ENSO winters. Therefore, for our cases, the latitudinal difference in active tropical convection appears to be most instrumental in enhancing the extratropical responses to the MJO-like dipole.

To add our explanation on the sensitivity of the Northern Hemisphere (NH) atmospheric response to northward migration of tropical forcings, we have obtained the correlation maps of area-averaged OLR and 200 hPa geopotential height (Fig. 7). The tropical regions of NH are divided into 20-degree longitude by 10-degree latitude bins between the equator and 20°N. Correlation coefficients between the global geopotential height anomalies are computed with reference to the OLR in each bin. Among the 18 regions of each latitude bands, we selected 4 regions that represent Indian Ocean, western Pacific, central Pacific, and Atlantic Ocean, respectively. From Fig. 7a to 7d, left panel is the correlation with the convection centered at the equator and the right panel is the correlation with the convection close to the subtropics. In this figure, we will only focus on comparing the increase/decrease of the correlation coefficients by the northward shift of the tropical convection. Shaded regions are statistically significant regions at 95 % confidence level.

When the convection is located over the Indian Ocean (Fig. 7a), wave-like propagating pattern is initiated from the Indian Ocean to the downstream re-

gion of North America at both latitude bands with no significant increase of the correlation coefficient by northward migration of the tropical forcing. In Fig. 7b, there is quite large difference between the two latitude bands. The relationship with the mid-latitude circulation from the western Pacific near the equator is very weak, but it is greatly enhanced by northward movement of the tropical convection. And the in-

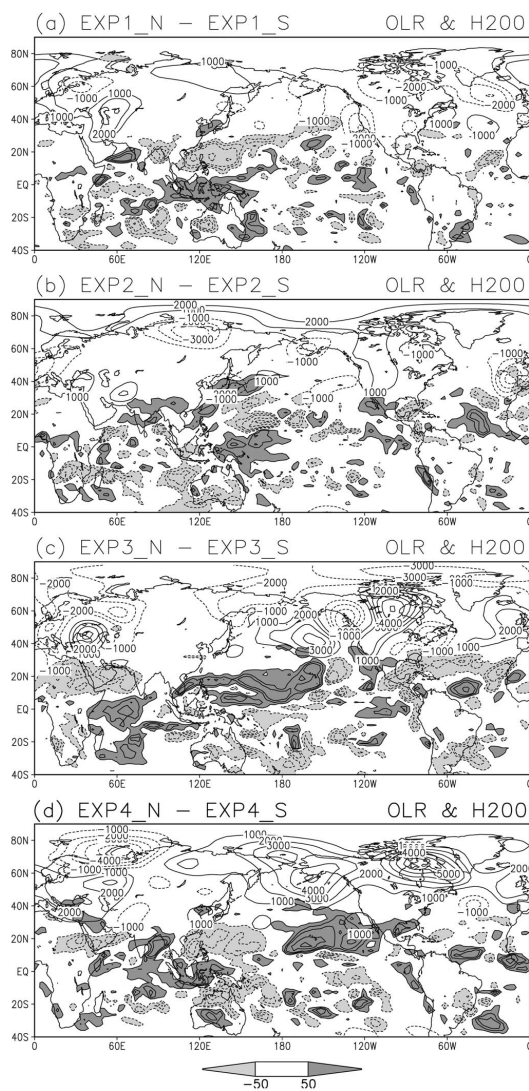


**Fig. 5.** Differences between the variance of experiments ( $_N$ ) and experiments ( $_S$ ) using OLR (in shading) and geopotential height at 200 hPa (H200) (in contour). Contour intervals are 1000  $\text{gpm}^2$  and shading intervals are 50  $\text{W/m}^2$ , respectively.

tensification only locates over the Asia-North Pacific-North America sector. In Fig. 7c, neither a signal nor an intensification can be detected since the SST near the dateline is in the condition of transition mode between the eastern and western hemisphere. Fig. 7d shows correlation from the tropical central Pacific with the upper-level circulation anomalies. PNA-like pattern is observed and this pattern becomes more robust when correlated with  $10^{\circ}$ - $20^{\circ}$ N band. In the case of the tropical convection over the Atlantic Ocean (Fig. 7e), the response from the tropics is regionally-confined to the America-Atlantic Ocean sectors and it is hard to find the difference in the magnitude of the correlation coefficient by the movement of convection from the south to the north.

From Fig. 7, it is suggested that the enhanced convection at the north of the tropical Pacific ( $10^{\circ}$ - $20^{\circ}$ N band) can induce large difference over the extratropics mainly over Asia-North Pacific-North America sectors. The extratropical response over the Indian Ocean and Atlantic Ocean showed global-scale propagating structure and regionally-confined structure, respectively, but there was little change in the

magnitude of the correlation coefficient by the northward migration.

## 6. Summary and Conclusion

The present study aims to explain the cause of the contrast in extratropical height variability between opposite phases of ENSO, which is suggested in the study of Moon and Ha (2002). We have used atmospheric general circulation model to verify the effect of tropical forcing on the extratropical circulation using idealized MJO-like heating anomalies centered at the equator and 10 degree north, respectively. To find out the sensitivity of the extratropical circulation anomalies by the longitudinal location of the tropical convection, correlation coefficient of area-averaged OLR and geopotential height is also obtained.

From the observation data from 1979 to 2000, the interannual variability of MJO and MJO-associated extratropical circulation during boreal winter showed significant contrast between El Niño and La Niña years. In La Niña events, the MJO convective maximum mostly activates at the northern periphery

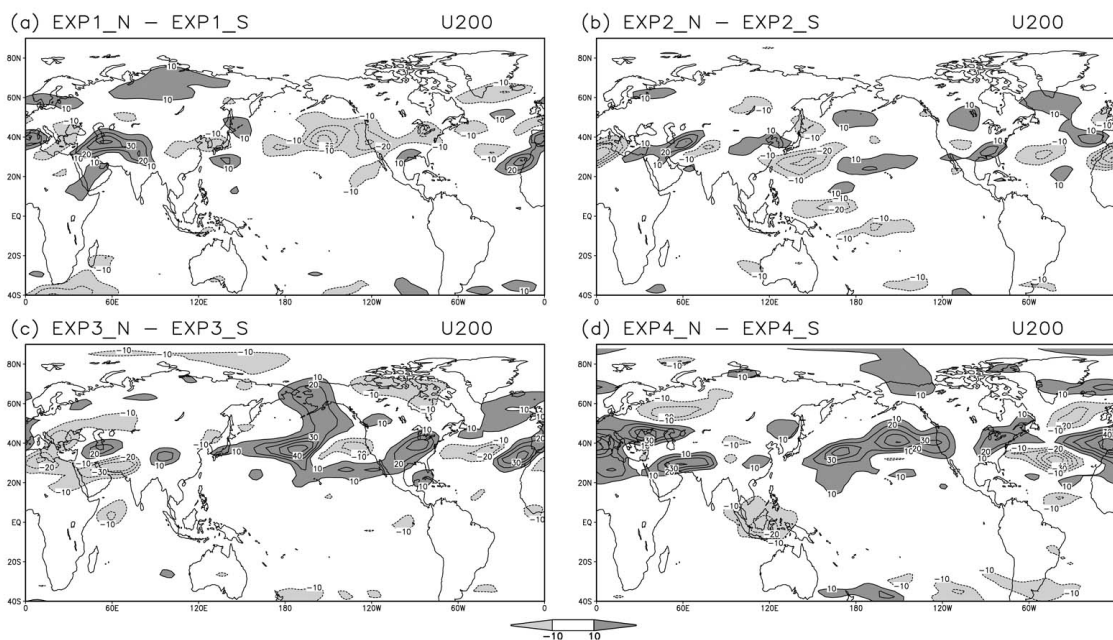


**Fig. 6.** Differences between the variance of experiments (N) and experiments (S) using zonal wind at 200 hPa (U200). Contour intervals are  $10 \text{ (m/s)}^2$  and values greater than  $10 \text{ (m/s)}^2$  are shaded.

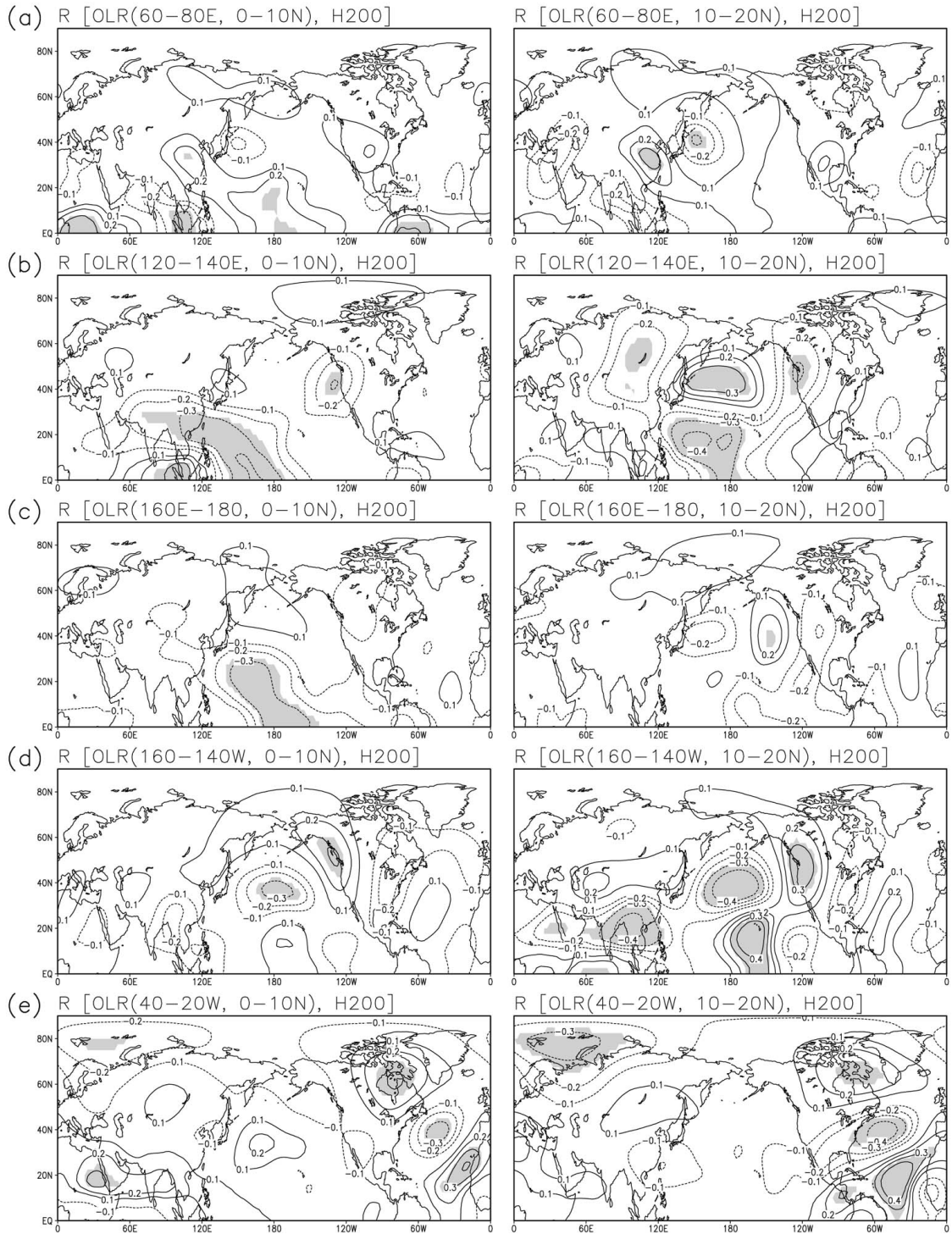


**Fig. 7.** Correlation coefficient between area-averaged OLR and geopotential height at 200 hPa. Contour interval is 0.1 and the shaded regions in the anomaly map indicate statistically significant regions of 95 % significance level.

of the climatological mean variance and the variability of extratropical height is greatly intensified especially over the north Pacific-North America sector. On the other hand, the convective area extends and intensifies to eastern Pacific in El Niño events as it has been already mentioned by the previous studies (Slingo *et al.* 1997; Hendon *et al.*, 1999). The MJO-associated extratropical height variability is significantly weakened during El Niño which seems to be caused by the trapped convective activity to the equator and Southern Hemisphere.

The simulation of the MJO-like convection and the response of the extratropical circulation is produced to be in good accordance with the observation, suggesting that the extratropical circulation has coherent life cycle of eastward evolution in phase with the tropical heating and cooling anomalies which mimic MJO.

As an effort to explain the cause of the difference in the magnitude of MJO-associated extratropical height variability between El Niño and La Niña years, idealized heating experiments have been performed. The response of the NH atmospheric circulation revealed obvious discrepancy in their variability over the Asia-Pacific-North America sectors when the northward migration of tropical heating anomalies locate in the tropical Pacific. Contrary to the result of Geisler *et al.* (1985), the simulated extratropical circulation was sensitive to the tropical heating displacement both in longitudinal and latitudinal directions in our study. From the analysis of correlation between area-averaged OLR and 200 hPa geopotential height in intraseasonal time scale, it is clearly identified when the tropical convection is disturbed to the north in the tropical Pacific, the extratropical circulation responds susceptibly especially over the Asia-North Pacific-North America sectors.

The enhanced convection at the north of the tropical Pacific (10°-20°N band) induces large upper-level zonal wind as well as the vorticity anomalies by the upper-level divergence reaching to the subtropics. The enhanced subtropical divergence/convergence system can act as a bridge between the tropical heating and extratropical circulation system. Thus the northward migration of the tropical con-

vection triggers the extratropical circulation anomalies by the subtropical divergence/convergence system as a main source for the mid-latitude response.

*Acknowledgement.* This research is supported by a project, “metri-2007-B-5”.

## REFERENCES

- Branstator, G., 1983: Horizontal Energy propagation in a Barotropic Atmosphere with Meridional and Zonal Structure. *J. Atmos. Sci.*, **40**, 1689-1708.
- \_\_\_\_\_, 2003: Remote response to tropical heating via the subtropical jet waveguide. 14<sup>th</sup> conference on atmospheric and oceanic fluid dynamics, 9-13 June 2003, San Antonio, Texas.
- Collins, W. D., P. J. Rasch, B. A. Boville, J. J. Hack, J. R. McCaa, D. L. Williamson, and B. P. Briegleb, 2006: The formulation and atmospheric simulation of the Community Atmosphere Model version 3 (CAM3). *J. Climate*, **19**, 2144-2161.
- Duchon, C. E., 1979: Lanczos filter in one and two dimensions. *J. Appl. Meteor.*, **18**, 1016-1022.
- Ferranti, L., T. N. Palmer, F. Molteni, and E. Klinker, 1990: Tropical-extratropical interaction associated with the 30-60 day oscillation and its impact on medium and extended range prediction. *J. Atmos. Sci.*, **47**, 2177-2199.
- Frankignoul, C., 1985: Sea surface temperature anomalies, planetary waves, and air/sea feedback in the middle latitudes. *Rev. Geophys.*, **23**, 357-390.
- Geisler, M. L., Blackmon, G. T. Bates, and S. Munoz, 1985: Sensitivity of January climate response to the magnitude and position of equatorial Pacific sea surface temperature anomalies. *J. Atmos. Sci.*, **42**, 1037-1049.
- Held, I. M., and I.-S. Kang, 1987: Barotropic models of the extratropical response to El Niño. *J. Atmos. Sci.*, **44**, 3576-3586.
- Hendon, H. H., and M. L. Salby, 1999: Interannual variation of the Madden-Julien oscillation during austral summer. *J. Climate*, **12**, 2538-2550.
- Hoerling, M. P., and M. Ting, 1994: Organization of extratropical transients during El Niño. *J. Climate*, **7**, 745-766.
- Hoskins, B. J., and D. J. Karoly, 1981: The steady linear response of a spherical atmosphere to thermal and orographic forcing. *J. Atmos. Sci.*, **38**, 1179-1196.
- Kiladis, G. N., and K. M. Weickmann, 1992: Circulation anomalies associated with tropical convection during northern winter. *Mon. Wea. Rev.*, **120**, 1900-1923.
- Knutson, T. R., and K. M. Weickmann, 1987: 30-60 day

- atmospheric oscillations: Composite life cycles of convection and circulation anomalies. *Mon. Wea. Rev.*, **115**, 1407-1436.
- Lau, K. M., and T. J. Philips, 1986: Coherent fluctuations of extratropical geopotential height and tropical convection in intraseasonal time scales. *J. Atmos. Sci.*, **43**, 1164-1181.
- Madden, R. A., and P. R. Julien, 1972: Description of global-scale circulation cells in the tropics with a 40-50 day period. *J. Atmos. Sci.*, **29**, 1109-1123.
- Moon, J. Y., and K. J. Ha, 2002: Coherent life cycle of intraseasonal tropical convection and extratropical circulation during El Niño and La Niña years: Diagnostic study. *J. Korean Meteor. Soc.*, **38**, 547-563.
- \_\_\_\_\_, B. Wang, and K. J. Ha, 2005: Coherent Life Cycle of Intraseasonal Tropical Convection and Extratropical Circulation during El Niño and La Niña years: GCM Study. *J. Korean Meteor. Soc.*, **41**, 201-216.
- Nitta, Ts., 1987: Convective activities in the tropical western Pacific and their impact of the Northern hemisphere summer circulation. *J. Meteor. Soc. Japan*, **65**, 373-390.
- Opsteegh, J. D., and H. M. Van den Dool, 1980: Seasonal differences in the stationary response of a linearized primitive equation model: Prospects for long-range weather forecasting? *J. Atmos. Sci.*, **37**, 2169-2185.
- Park, C. K., M. J. Suarez, and S. D. Schubert, 1995: Response of the zonally asymmetric flow to time-dependent tropical heating. *J. Atmos. Sci.*, **52**, 3738-3756.
- Rui, H., and B. Wang, 1989: Development characteristics and dynamic structure of tropical intraseasonal convection anomalies. *J. Atmos. Sci.*, **47**, 357-379.
- Sardeshmukh, P. D., and B. J. Hoskins, 1988: The generation of global rotational flow by steady idealized tropical divergence. *J. Atmos. Sci.*, **45**, 1228-1251.
- Shukla, J., 1981: Dynamical predictability of monthly means. *J. Atmos. Sci.*, **38**, 2547-2572.
- \_\_\_\_\_, and J. M. Wallace, 1983: Numerical Simulation of the Atmospheric Response to Equatorial Pacific Sea Surface Temperature Anomalies. *J. Atmos. Sci.*, **40**, 1613-1630.
- Simmons, A. J., 1982: The forcing of stationary wave motion by tropical diabatic heating. *Quart. J. Roy. Meteor. Soc.*, **108**, 503-534.
- Slingo, J. M., D. P. Rowell, K. R. Sperber, and F. Nortley, 1999: On the predictability of the interannual behaviour of the Madden-Julien oscillation and its relationship with El Niño. *Quart. J. Roy. Meteor. Soc.*, **125**, 583-609.
- Ting, M.-F., and I. M. Held, 1990: The stationary wave response to a tropical SST anomaly in an idealized GCM. *J. Atmos. Sci.*, **47**, 2546-2566.
- \_\_\_\_\_, and P. D. Sardeshmukh, 1993: Factors Determining the Extratropical Response to Equatorial Diabatic Heating Anomalies. *J. Atmos. Sci.*, **50**, 907-918.
- Wallace, J. M., and D. S. Gutzler, 1981: Teleconnections in the geopotential height field during the northern hemisphere winter. *Mon. Wea. Rev.*, **109**, 784-812.
- Weickmann, K. M., 1983: Intraseasonal circulation and outgoing longwave radiation modes during northern winter. *Mon. Wea. Rev.*, **111**, 1838-1858.